Storage and retrieval of vector optical solitons via double electromagnetically induced transparency

Yang Chen,[1] Zhiming Chen,[1] and Guoxiang Huang[1,2,*]

[1]*State Key Laboratory of Precision Spectroscopy and Department of Physics, East China Normal University, Shanghai 200062, China*

[2]*ECNU-NYU Joint Physics Research Institute at NYU-Shanghai, Shanghai 200062, China*

(Received 17 July 2014; published 17 February 2015)

We propose a scheme to realize storage and retrieval of two-component optical soliton in a coherent atomic system. The system under consideration is a cold, lifetime-broadened four-level atomic gas with a tripod configuration working at the condition of double electromagnetically induced transparency. We show that due to the existence of two dark states, the optical absorption of the probe pulse can be largely reduced. In addition, the two orthogonal polarization components of the probe pulse with a form of vector optical soliton cannot only be slowed down substantially but also be stored and retrieved robustly by switching a control laser field off and on. We also show that it is possible to achieve a memory of N-component optical soliton by using the N dark states in a $(N+1)$-pod system ($N>2$). The results reported here may have promise in applications for light information processing in a weak nonlinear regime.

DOI: 10.1103/PhysRevA.91.023820 PACS number(s): 42.65.Tg, 05.45.Yv

I. INTRODUCTION

In recent years, much attention has been paid to the investigation of light storage and retrieval, which is very crucial for the realization of optical information processing. One of the important techniques for realizing light storage and retrieval is the use of electromagnetically induced transparency (EIT), which is a quantum interference effect typically occurring in a three-level atomic system [1]. Due to the existence of a dark state, a probe laser field can be stored in atoms and retrieved by manipulating a control laser field [2].

However, nearly all studies up to now on light storage and retrieval via EIT have been carried out in a linear regime. It is well known that a linear probe pulse in an EIT system suffers a spreading and attenuation due to the existence of dispersion, which may result in a serious distortion for retrieved pulse. For practical applications of optical memory, it is desirable to obtain a probe pulse that is robust during its storage and retrieval (i.e., with a high fidelity). A preliminary analysis shows that a weak optical soliton pulse can be stored and retrieved in three-level atomic systems via a single EIT [3,4].

In this article, we propose a scheme to realize the storage and retrieval of vector optical soliton (VOS) in a cold, lifetime-broadened four-level atomic system with a tripod configuration and working under the condition of double electromagnetically induced transparency (DEIT). We show that due to the existence of the DEIT and hence two dark states, the optical absorption of the probe pulse can be largely reduced. In addition, the two orthogonal polarization components of the VOS cannot only be slowed down substantially but also be stored and retrieved robustly by switching a control field off and on. We further show that it is possible to realize the storage and retrieval of N-component optical soliton by using the N dark states in a $(N+1)$-pod system ($N>2$). The result reported here provides the possibility of the high-fidelity bit memory and hence may have promise in applications in light information processing in a weak nonlinear regime.

Before preceding, we note that DEIT has been explored in many previous studies, which showed that two probe fields can be made transparent by the use of control field [5–10]. Additionally, the storage and retrieval of the two probe fields in DEIT systems have also been demonstrated experimentally [11–15]. However, our work is different from Refs. [5–10], where only linear DEIT was investigated. Furthermore, our work is also at variance with Refs. [11–15], where only the memory of two probe pulses in the linear propagation regime was explored. In contrast with these studies, in our work not only a nonlinear DEIT but also the storage and retrieval of two solitonic probe pulses in nonlinear propagation regime are explored.

The article is arranged as follows. In Sec. II, the physical model under study is described. In Sec. III, a derivation of coupled NLS equations controlling the evolution of envelopes of the two polarization components of the probe field is given, and an ultraslow VOS solution is also presented. In Sec. IV, storage and retrieval of the VOS are investigated in detail and a theoretical explanation is also presented. In Sec. V, the storage and retrieval of N-component optical solitons is discussed. Finally, the last section contains a summary of the main results of our work.

II. MODEL

We consider a cold, lifetime-broadened atomic gas with a tripod-type level configuration, interacting resonantly with a pulsed probe laser field with two orthogonal circular-polarized components (with half-Rabi frequency Ω_{p1} and Ω_{p2}, respectively), and a linear-polarized, strong continuous-wave control laser field (with half-Rabi frequency Ω_c). The two polarization components of the probe field drive, respectively, the transitions from $|4\rangle \leftrightarrow |1\rangle$ and $|4\rangle \leftrightarrow |2\rangle$, while the control field drives the transitions from $|4\rangle \leftrightarrow |3\rangle$ [see Fig. 1(a)]. A possible arrangement of experimental apparatus is shown in Fig. 1(b).

For simplicity, we assume both the probe and control fields propagate along the z direction. Then the electric field of the system can be expressed as $\mathbf{E} = (\hat{\epsilon}_+\mathcal{E}_{p^+} + \hat{\epsilon}_-\mathcal{E}_{p^-})\exp[i(k_p z - \omega_p t)] + \hat{\epsilon}_c\mathcal{E}_c\exp[i(k_c z - \omega_c t)] + \text{c.c.}$

*gxhuang@phy.ecnu.edu.cn

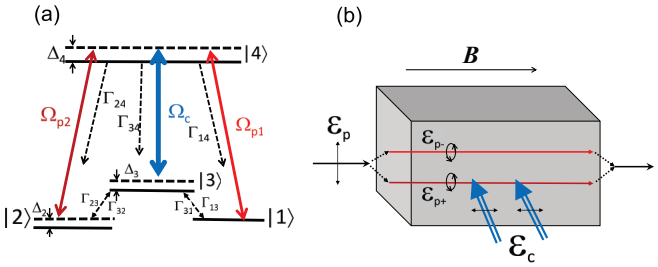

FIG. 1. (Color online) (a) Energy-level diagram and excitation scheme of the four-level tripod atomic system. Ω_{p1} and Ω_{p2} are the half-Rabi frequencies of two polarization components of the probe field, which couple, respectively, to the levels $|4\rangle \rightarrow |1\rangle$ and $|4\rangle \rightarrow |2\rangle$. The levels $|3\rangle$ and $|4\rangle$ are coupled by the control field with half-Rabi frequency Ω_c. Γ_{14}, Γ_{24}, and Γ_{34} are, respectively, the spontaneous emission decay rates from $|4\rangle$ to $|1\rangle$, $|4\rangle$ to $|2\rangle$, and $|4\rangle$ to $|3\rangle$. Δ_4, Δ_3, and Δ_2 are detunings. Γ_{13}, Γ_{31}, Γ_{23}, and Γ_{32} are, respectively, the rates of incoherent population transfer between $|3\rangle$ and $|1\rangle$, and between $|3\rangle$ and $|2\rangle$. (b) Possible arrangement of experimental apparatus. $\mathcal{E}_c$ is the control field and $\mathcal{E}_{p^-}$ and $\mathcal{E}_{p^+}$ are the two circular-polarized components of the probe field $\mathcal{E}_p$, respectively. **B** is an applied magnetic that induces a Zeeman splitting of the lower levels.

Here $\hat{\epsilon}_+ = (\hat{\mathbf{x}} + i\hat{\mathbf{y}})/\sqrt{2}$ ($\hat{\epsilon}_- = (\hat{\mathbf{x}} - i\hat{\mathbf{y}}/\sqrt{2})$) is the probe-field unit vector of the circular-polarized component with the envelope $\mathcal{E}_{p^+}$ ($\mathcal{E}_{p^-}$), which drives the transition $|2\rangle \leftrightarrow |4\rangle$ ($|1\rangle \leftrightarrow |4\rangle$); $\hat{\mathbf{x}}$ ($\hat{\mathbf{y}}$) is the unit vector along the x (y) direction; $\hat{\epsilon}_c$ is the unit vector of the control field with the envelope $\mathcal{E}_c$; $k_p = \omega_p/c$ ($k_c = \omega_c/c$) is the wave number of the probe (control) field before entering the atomic gas.

The Hamiltonian of the system in the interaction picture is given by

$$H_{\rm int} = -\hbar\left(\sum_{j=1}^{4}\Delta_j|j\rangle\langle j| + \Omega_{p1}|4\rangle\langle 1| + \Omega_{p2}|4\rangle\langle 2| + \Omega_c|4\rangle\langle 3| + \text{H.c.}\right), \tag{1}$$

with $\Delta_1 = 0$, $\Delta_2 = (E_1 - E_2)/\hbar$, $\Delta_3 = \omega_p - \omega_c - (E_3 - E_1)/\hbar$, and $\Delta_4 = \omega_p - (E_4 - E_1)/\hbar$. Here E_j is the energy eigenvalue of the level $|j\rangle$ ($j = 1,2,3,4$); Ω_{p1} (Ω_{p2}) is the half-Rabi frequency of the $\mathcal{E}_{p^-}$ ($\mathcal{E}_{p^+}$) component of the probe field; Ω_c is the half-Rabi frequency of the control field.

The motion of atoms is governed by the Bloch equation [16],

$$i\hbar\left(\frac{\partial}{\partial t} + \Gamma\right)\sigma = [H_{\rm int},\sigma], \tag{2}$$

where σ is a 4×4 density matrix in the interaction picture, and Γ is a 4×4 relaxation matrix describing the spontaneous emission and dephasing of the system. The definitions of Ω_α ($\alpha = p1,p2,c$) and the explicit expressions of Eq. (2) are presented in Appendix A.

The evolution of the electric field in the system is controlled by the Maxwell equation,

$$\nabla^2\mathbf{E} - \frac{1}{c^2}\frac{\partial^2\mathbf{E}}{\partial t^2} = \frac{1}{\varepsilon_0 c^2}\frac{\partial^2\mathbf{P}}{\partial t^2}, \tag{3}$$

with $\mathbf{P} = \mathcal{N}_a\{\mathbf{p}_{14}\sigma_{41}\exp[i(k_pz - \omega_pt)] + \mathbf{p}_{24}\sigma_{42}\exp[i(k_pz - \omega_pt)] + \mathbf{p}_{34}\sigma_{43}\exp[i(k_cz - \omega_ct)] + \text{c.c.}\}$. Under a slowly varying envelope approximation, we obtain the equations for Ω_α ($\alpha = p1,p2,c$),

$$i\left(\frac{\partial}{\partial z} + \frac{1}{c}\frac{\partial}{\partial t}\right)\Omega_{p1} + \kappa_{14}\sigma_{41} = 0, \tag{4a}$$

$$i\left(\frac{\partial}{\partial z} + \frac{1}{c}\frac{\partial}{\partial t}\right)\Omega_{p2} + \kappa_{24}\sigma_{42} = 0, \tag{4b}$$

$$i\left(\frac{\partial}{\partial z} + \frac{1}{c}\frac{\partial}{\partial t}\right)\Omega_{c} + \kappa_{34}\sigma_{43} = 0, \tag{4c}$$

where $\kappa_{14} = \mathcal{N}_a\omega_p|\mathbf{p}_{14}|^2/(2\varepsilon_0 c\hbar)$, $\kappa_{24} = \mathcal{N}_a\omega_p|\mathbf{p}_{24}|^2/(2\varepsilon_0 c\hbar)$, and $\kappa_{34} = \mathcal{N}_a\omega_c|\mathbf{p}_{34}|^2/(2\varepsilon_0 c\hbar)$, with $\mathcal{N}_a$ the atomic density and c the light speed in vacuum. Note that for simplicity we have assumed both the probe and control fields have large beam radius in x and y directions so that the diffraction effect representing by the term $(\partial^2/\partial x^2 + \partial^2/\partial y^2)\Omega_\alpha$ are negligible.

III. ULTRASLOW VECTOR OPTICAL SOLITONS

A. Nonlinear envelope equations

We first use the standard method of multiple scales developed for EIT-like resonant atomic systems [17] to derive nonlinear envelope equations for the two orthogonal components of the probe pulse based on the nonlinearly coupled Maxwell-Bloch (MB) Eqs. (A1) and (4) by assuming a constant control field. To this end, we take the asymptotic expansions $\sigma_{jj} = \sigma_{jj}^{(0)} + \epsilon\sigma_{jj}^{(1)} + \epsilon^2\sigma_{jj}^{(2)} + \epsilon^3\sigma_{jj}^{(3)} + \cdots (j = 1,2,3,4)$, $\sigma_{jl} = \sigma_{jl}^{(0)} + \epsilon\sigma_{jl}^{(1)} + \epsilon^2\sigma_{jl}^{(2)} + \epsilon^3\sigma_{jl}^{(3)} + \cdots (j = 2,3,4; l = 1,2,3)$, and $\Omega_{pl} = \epsilon\Omega_{pl}^{(1)} + \epsilon^2\Omega_{pl}^{(2)} + \epsilon^3\Omega_{pl}^{(3)} + \cdots (l = 1,2)$. Here $\sigma_{jj}^{(0)}$ is the initial population distribution prepared in the state $|j\rangle$, $\sigma_{jl}^{(0)}$ is the initial coherence related to the state $|j\rangle$ and the state $|l\rangle$, and ϵ is a dimensionless small parameter characterizing the typical amplitude of Ω_{p1} and Ω_{p2}. To obtain a valid expansion for the nonlinear evolution of the system, all quantities on the right-hand side of the expansion are considered as functions of the multiscale variables $z_l = \epsilon^l z$ ($l = 0,1,2$), and $t_l = \epsilon^l t$ ($l = 0,1$) [17].

Substituting the above expansion to the MB Eqs. (A1), (4a), and (4b) and comparing the coefficients of ϵ^l ($l = 1,2,3...$), we obtain a set of linear but inhomogeneous equations which can be solved order by order. At zero order, the solution reads

$$\sigma_{11}^{(0)} = \frac{J_{12}G_2 - J_{22}G_1}{J_{12}J_{21} - J_{11}J_{22}}, \tag{5a}$$

$$\sigma_{22}^{(0)} = \frac{J_{21}G_1 - J_{11}G_2}{J_{12}J_{21} - J_{11}J_{22}}, \tag{5b}$$

$$\sigma_{44}^{(0)} = \frac{X_1 - i\Gamma_{31} - X_1\sigma_{11}^{(0)} - X_2\sigma_{22}^{(0)}}{X_4}, \tag{5c}$$

$$\sigma_{43}^{(0)} = \frac{-\Omega_c\left(1 - \sigma_{11}^{(0)} - \sigma_{22}^{(0)} - 2\sigma_{44}^{(0)}\right)}{(\omega + d_{43})}, \tag{5d}$$

where $\sigma_{33}^{(0)} = 1 - \sigma_{11}^{(0)} - \sigma_{22}^{(0)} - \sigma_{44}^{(0)}$; X_j ($j = 1,2,4$), G_l ($l = 1,2$), J_{jk} ($j,k = 1,2, j \neq k$) are given in Appendix B. Note that the populations in the level $|3\rangle$ and $|4\rangle$ come from the

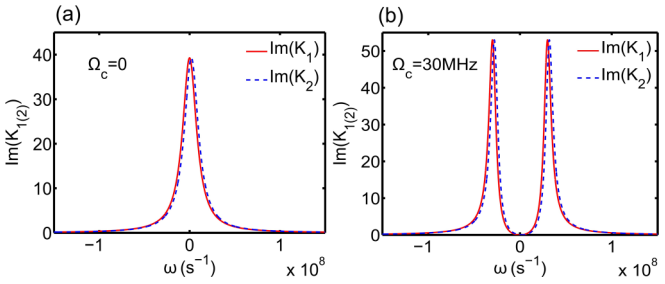

FIG. 2. (Color online) DEIT in the tripod system. Im(K_1) (solid line) and Im(K_2)(dashed line) are the absorption spectra of the two polarization components of the probe pulse as functions of ω. (a) The case without EIT ($\Omega_c = 0$). (b) The case with DEIT ($\Omega_c = 30$ MHz), where a transparency window opens for both Im(K_1) and Im(K_2).

incoherent population transfer (i.e., Γ_{31} and Γ_{32}). We assume both Γ_{31} and Γ_{32} are small so that the populations in $|3\rangle$ and $|4\rangle$ are negligible.

At the first order, we obtain the solution $\Omega_{p1}^{(1)} = F_1 \exp(i\theta_1)$ and $\Omega_{p2}^{(1)} = F_2 \exp(i\theta_2)$ with $\theta_{1(2)} = K_{1(2)}(\omega) z_0 - \omega t_0$ [18] and $F_{1(2)}$ the envelope function of the slow variables z_1, z_2, and t_1. K_1 and K_2 are linear dispersion relations, given by

$$K_1(\omega) = \frac{\omega}{c} + \kappa_{14} \frac{(\omega + d_{31})\left(\sigma_{11}^{(0)} - \sigma_{44}^{(0)}\right) + \Omega_c \sigma_{43}^{*(0)}}{D_1(\omega)}, \quad (6a)$$

$$K_2(\omega) = \frac{\omega}{c} + \kappa_{24} \frac{(\omega + d_{32})\left(\sigma_{22}^{(0)} - \sigma_{44}^{(0)}\right) + \Omega_c \sigma_{43}^{*(0)}}{D_2(\omega)}, \quad (6b)$$

with $D_j(\omega) = |\Omega_c|^2 - (\omega + d_{3j})(\omega + d_{4j})$ ($j = 1,2$). We see that the linear dispersion relation has two branches, belonging, respectively, to the two orthogonal polarization components of the probe field. The explicit expressions of $\sigma_{jl}^{(1)}$ are presented in Appendix C.

Shown in Fig. 2 are absorption spectra Im(K_1) (solid line) and Im(K_2) (dashed line) as functions of ω. Figures 2(a) and 2(b) are, respectively, for the absence ($\Omega_c = 0$) and the presence ($\Omega_c = 30$ MHz) of the control field. We see that when $\Omega_c = 0$ both polarization components of the probe pulse have large absorption [Fig. 2(a)] (i.e., no EIT); however, in the presence of Ω_c a transparency window is opened in both Im(K_1) and Im(K_2) [Fig. 2(b)]. In this situation, the two polarization components of the probe pulse may propagate in the present resonant atomic ensemble with negligible absorption (i.e., DEIT). The occurrence of the DEIT is due to the quantum interference effect induced by the control field, which allows the existence of two dark states (i.e., the upper state $|4\rangle$ is not involved),

$$|D_1\rangle = \Omega_c |1\rangle - \Omega_{p1} |3\rangle, \quad (7a)$$

$$|D_2\rangle = \Omega_c |2\rangle - \Omega_{p2} |3\rangle, \quad (7b)$$

for the Hamiltonian (1). Note that when plotting Fig. 2, the model and system parameters given in Appendix A have been used. In addition, we have taken $\Delta_3 = \Delta_4 = 0$, $\Delta_2 = 2$ MHz (here a larger Δ_2 is chosen for distinguishing the curves in the figure), $\mathcal{N}_a = 5.51 \times 10^{11} \mathrm{cm}^{-3}$, and hence $\kappa_{14} \approx \kappa_{24} \approx 1.5 \times 10^{10} \mathrm{cm}^{-1}\mathrm{s}^{-1}$.

To study the weak nonlinear effect of the system, we must go to high-order approximations. At second order, we obtain $i[\partial F_l/\partial z_1 + (1/V_{gl})\partial F_l/\partial t_1] = 0$ ($l = 1,2$), with $V_{gl} = 1/K_{1l}$ ($K_{l1} \equiv \partial K_l/\partial\omega$) the group velocity of the lth polarization component of the probe pulse. The second-order solution is presented in Appendix D.

With the above result we proceed to the third order. The divergence-free condition in this order yields the nonlinear envelope equations for F_1 and F_2:

$$i\frac{\partial F_1}{\partial z_2} - \frac{1}{2}K_{12}\frac{\partial^2 F_1}{\partial t_1^2} - (W_{11}|F_1|^2 e^{-2\bar{\alpha}_1 z_2} + W_{12}|F_2|^2 e^{-2\bar{\alpha}_2 z_2})F_1 = 0, \quad (8a)$$

$$i\frac{\partial F_2}{\partial z_2} - \frac{1}{2}K_{22}\frac{\partial^2 F_2}{\partial t_1^2} - (W_{21}|F_1|^2 e^{-2\bar{\alpha}_1 z_2} + W_{22}|F_2|^2 e^{-2\bar{\alpha}_2 z_2})F_2 = 0, \quad (8b)$$

where $\bar{\alpha}_l = \epsilon^{-2}\alpha_l = \epsilon^{-2}\mathrm{Im}(K_l)$ is absorption coefficient, $K_{l2} = \partial^2 K_l/\partial\omega^2$ is group-velocity dispersion coefficient, and W_{ll} is a nonlinear coefficient characterizing self-phase modulation (SPM) of the lth polarization component of the probe field; W_{12} and W_{21} are nonlinear coefficients characterizing cross-phase modulations (CPMs) between the two polarization components. The explicit expressions of all these quantities are given in Appendix E.

B. Ultraslow vector optical solitons

We now consider possible VOS solutions of the coupled nonlinear Eqs. (8a) and (8b). Notice that these equations have generally complex coefficients. However, due to the existence of the DEIT the imaginary parts of these complex coefficients are very small and can be taken as perturbations (see the example given below). For a transparent physical analysis, these small imaginary parts are neglected in analytical calculations but will be included in numerical simulations.

By defining $s = z/L_D$, $\sigma = (t - z/V_g)/\tau_0$, $u_1 = (\Omega_{p1}/U_0)\exp(-iK_1 z)$, and $u_2 = (\Omega_{p2}/U_0)\exp(-iK_2 z)$, Eqs. (8a) and (8b) are converted into the dimensionless form,

$$i\left(\frac{\partial}{\partial s} + g_{A1}\right)u_1 + ig_\delta\frac{\partial u_1}{\partial\sigma} - \frac{g_{D1}}{2}\frac{\partial^2 u_1}{\partial\sigma^2} - (g_{11}|u_1|^2 + g_{12}|u_2|^2)u_1 = 0, \quad (9a)$$

$$i\left(\frac{\partial}{\partial s} + g_{A2}\right)u_2 - ig_\delta\frac{\partial u_2}{\partial\sigma} - \frac{g_{D2}}{2}\frac{\partial^2 u_2}{\partial\sigma^2} - (g_{21}|u_1|^2 + g_{22}|u_2|^2)u_2 = 0, \quad (9b)$$

with $g_{Al} = \alpha_l L_D$ ($l = 1,2$), $g_\delta = \mathrm{sign}(\delta)L_D/L_\delta$, $g_{D1} = K_{12}/|K_{22}|$, $g_{D2} = \mathrm{sgn}(K_{22})$, $g_{lm} = W_{lm}/|W_{22}|$ ($l,m = 1,2$), $\delta = (1/V_{g1} - 1/V_{g2})/2$, and $V_g = 2V_{g1}V_{g2}/(V_{g1} + V_{g2})$. Here $L_D = \tau_0^2/|K_{22}|$ is the characteristic dispersion length, $L_\delta = \tau_0/|\delta|$ is the characteristic length for group-velocity mismatch, and τ_0 is the characteristic pulse length. Since our aim is to obtain VOS solutions, in Eqs. (9a) and (9b) we have assumed $L_D = L_{\mathrm{NL}}$, with $L_{\mathrm{NL}} = 1/(U_0^2|W_{22}|)$ being characteristic nonlinear length of the system.

For the system parameters given in Appendix A, and when selecting $\Delta_4 = 6.0 \times 10^8$ Hz, $\Delta_3 = 2.0 \times 10^6$ Hz, $\Delta_2 = 1.0 \times 10^4$ Hz, $\Gamma_{31} \approx \Gamma_{32} = 100$ Hz, $\Gamma_{13} \approx \Gamma_{23} = \Gamma_3/2$, $\Gamma_{14} \approx \Gamma_{24} \approx \Gamma_{34} = \Gamma_4/3$, $\kappa_{14} \approx \kappa_{24} = 1.5 \times 10^{10}$ cm^{-1}s^{-1}, and $\Omega_c = 2.4 \times 10^8$ Hz, we obtain the numerical values of the complex coefficients in Eqs. (8a) and (8b) evaluating at $\omega = 0$ (i.e., at the center frequency of the probe field), which are $K_1 = (0.26595 + i0.00031)$ cm^{-1}, $K_2 = (0.26460 + i0.00031)$ cm^{-1}, $K_{11} = (1.35851 + i0.00184) \times 10^{-7}$ cm^{-1}s, $K_{21} = (1.35821 + i0.00183) \times 10^{-7}$ cm^{-1}s, $K_{12} = (2.90860 + i0.0965) \times 10^{-15}$ cm^{-1}s^2, $K_{22} = (2.90752 + i0.0964) \times 10^{-15}$ cm^{-1}s^2, $W_{11} = (2.26869 + i0.07441) \times 10^{-16}$ cm^{-1}s^2, $W_{12} = (2.22029 + i0.07440) \times 10^{-16}$ cm^{-1}s^2, $W_{21} = (2.22054 + i0.07427) \times 10^{-16}$ cm^{-1}s^2, and $W_{22} = (2.26821 + i0.07438) \times 10^{-16}$ cm^{-1}s^2. We see that the imaginary parts of these quantities are indeed much smaller than their relevant real parts, as expected above. The physical reason of such small imaginary parts comes from the DEIT effect induced by the control field. Additionally, all four Kerr coefficients W_{11}, W_{12}, W_{21}, W_{22} are very large (comparing with those, e.g., in optical fibers) and have the same order of magnitude, which is due to the DEIT and the symmetry of the tripod level configuration (i.e., the detunings of all the lower levels are taken to be small).

When taking $\tau_0 = 1.0 \times 10^{-7}$ s, we obtain $U_0 \approx 3.58 \times 10^7$ s^{-1}, and $L_D = 3.43$ cm. Furthermore, one has $L_\delta = 6874$ cm, which means that the group velocities of the two polarization components are matched well. The dimensionless coefficients read $g_\delta = 0.001$, $g_{D1} \approx 1$, $g_{D2} = 1$, and $g_{11} \approx g_{21} \approx g_{12} \approx g_{22} \approx 1$. When disregarding the small imaginary parts of the coefficients, Eqs. (9a) and (9b) become coupled nonlinear Schrödinger (NLS) equations. A bright-bright VOS solution is given by

$$u_1 = \nu_1 \mathrm{sech}(A_0\sigma + B_0 s)\exp[i(\varrho_1\sigma + \varsigma_1 s)], \quad (10a)$$

$$u_2 = \nu_2 \mathrm{sech}(A_0\sigma + B_0 s)\exp[i(\varrho_2\sigma + \varsigma_2 s)], \quad (10b)$$

if the parameters fulfill the condition $g_{22}g_{D1} = g_{12}g_{D2}$. We have defined $\varrho_1 = (B_0 + g_\delta A_0)/(g_{D1}A_0)$, $\varrho_2 = (B_0 - g_\delta A_0)/(g_{D2}A_0)$, $\varsigma_1 = -\varrho_1 g_\delta - g_{D1}(A_0^2 - \varrho_1^2)/2$, $\varsigma_2 = \varrho_2 g_\delta - g_{D2}(A_0^2 - \varrho_2^2)/2$, and $\nu_2 = [(g_{D1}A_0^2 - g_{11}\nu_1^2)/g_{12}]^{1/2}$. Here ν_1, A_0, B_0 are free parameters.

After returning to the original variables, we obtain

$$\Omega_{p1}(z,t) = \frac{1}{\tau_0}\sqrt{\left|\frac{\tilde{W}_{12}\tilde{K}_{22}}{\tilde{W}_{11}\tilde{W}_{22}}\right|}\mathrm{sech}\left[\frac{A_0}{\tau_0}\left(t - \frac{z}{\tilde{V}_g}\right) + \frac{B_0 z}{L_D}\right]e^{i\phi_1}, \quad (11a)$$

$$\Omega_{p2}(z,t) = \frac{1}{\tau_0}\sqrt{\left|\frac{A_0^2\tilde{W}_{22}\tilde{K}_{12}}{\tilde{W}_{12}\tilde{K}_{22}}\right| - 1}\sqrt{\left|\frac{\tilde{K}_{22}}{\tilde{W}_{22}}\right|} \times \mathrm{sech}\left[\frac{A_0}{\tau_0}\left(t - \frac{z}{\tilde{V}_g}\right) + \frac{B_0 z}{L_D}\right]e^{i\phi_2}. \quad (11b)$$

One sees that the CPM coefficient $\tilde{W}_{12}$ appears explicitly in the solution, which is a manifestation of the interaction between the two polarization components of the VOS.

The probe-field expression corresponding the VOS is given by

$$\mathbf{E}_p(z,t) = \left(\hat{\epsilon}_- \frac{\hbar}{|\mathbf{p}_{14}|\tau_0}\sqrt{\left|\frac{\tilde{W}_{12}\tilde{K}_{22}}{\tilde{W}_{11}\tilde{W}_{22}}\right|}e^{i\phi_1} + \hat{\epsilon}_+ \frac{\hbar}{|\mathbf{p}_{24}|\tau_0}\sqrt{\left|\frac{A_0^2\tilde{K}_{12}\tilde{W}_{22}}{\tilde{W}_{12}\tilde{K}_{22}}\right| - 1}\sqrt{\left|\frac{\tilde{K}_{22}}{\tilde{W}_{22}}\right|}e^{i\phi_2}\right)\mathrm{sech}\left[\frac{A_0}{\tau_0}\left(t - \frac{z}{\tilde{V}_g}\right) + \frac{B_0 z}{L_D}\right]e^{i(k_p z - \omega_p t - \omega t)} + \text{c.c.}, \quad (12)$$

where $\phi_1 = \tilde{K}_1 z + B_0|\tilde{K}_{22}|(t - z/\tilde{V}_g)/(A_0\tilde{K}_{12}\tau_0) - (z/L_D)(A_0^4\tilde{K}_{12}^2 - B_0^2\tilde{K}_{22}^2)/(2A_0^2|\tilde{K}_{22}|\tilde{K}_{12})$ and $\phi_2 = \tilde{K}_2 z + B_0(t - z/\tilde{V}_g)/(A_0\tau_0) - (z/L_D)(A_0^4 - B_0^2)/(2A_0^2)$, with A_0 and B_0 being two free parameters. We see that the envelopes of the two (circularly) polarized components of the VOS have the same propagating velocity $\tilde{V}_g/[1 - B_0\tilde{V}_g\tau_0/(A_0 L_D)]$.

With the above results, we obtain the propagating velocities of the two polarization components of the VOS,

$$\tilde{V}_{s1} = 2.45683 \times 10^{-4}\, c, \quad (13a)$$

$$\tilde{V}_{s2} = 2.45683 \times 10^{-4}\, c, \quad (13b)$$

when taking $A_0 = 2$ and $B_0 = 1$. We see that both V_{s1} and V_{s2} are ultraslow and matched. The ultraslow and matched propagating velocities are very crucial for the simultaneous memory of the two components of the VOS.

The threshold of the optical power density $P_{\max}$ for generating the VOS predicted above can be estimated by using Poynting's vector [17]. We have

$$P_{\max} \approx 1.33 \times 10^{-9}\ \text{W}. \quad (14)$$

Thus, to create the ultraslow optical solitons in the system very low input power is needed. The reason for such low generation power of the VOS is due to the giant Kerr nonlinearity (i.e., large SPM and CPM coefficients) produced by the DEIT effect.

IV. STORAGE AND RETRIEVAL OF VECTOR OPTICAL SOLITONS

A. Storage and retrieval of the two polarization components of the probe field

Fleischhauer and Lukin [19] demonstrated that it is possible to realize storage and retrieval of a probe optical pulse in a Λ-type three-level atomic system. First, by switching on a control field the probe pulse may propagate in the atomic system with nearly vanishing absorption. Then by slowly switching off the control field the probe pulse will disappear and get stored in the form of atomic coherence. Later on, by switching on the control field again the probe pulse will reappear. In recent years, such theoretical prediction has been verified successfully by a series of beautiful experiments [20–33].

However, the intensity of the probe pulse used in Ref. [19] and the studies carried out thereafter [20–33] is weak; i.e.,

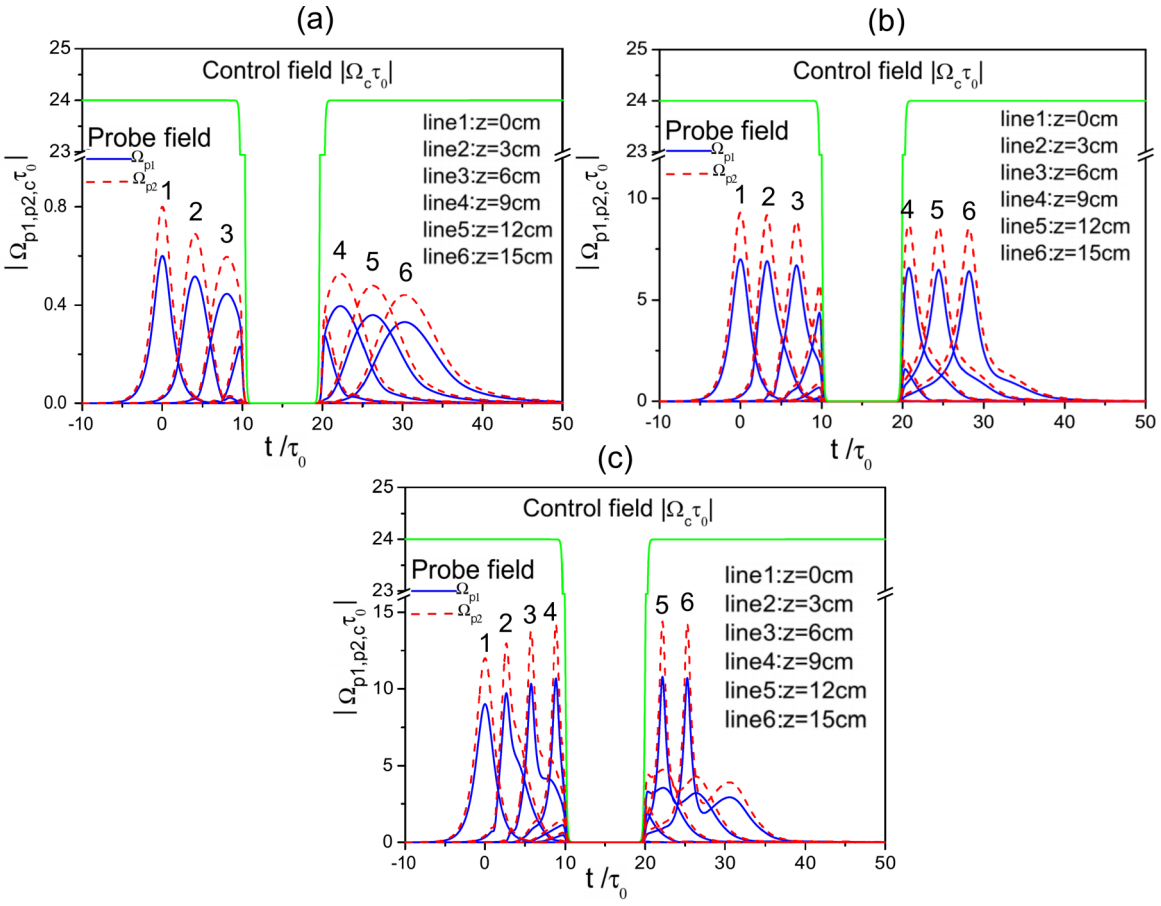

FIG. 3. (Color online) Storage and retrieval of two-component optical pulse in different dynamic regimes. Shown in each panel are profiles of $|\Omega_{p1}\tau_0|$ (blue solid line) and $|\Omega_{p2}\tau_0|$ (red dashed line) as functions of z and t for different input light intensity of the probe pulse. (a) Dispersion-dominant (i.e., linear) regime $[\Omega_{p1}(0,t)\tau_0 = 0.6\,\mathrm{sech}(t/\tau_0), \Omega_{p2}(0,t)\tau_0 = 0.8\,\mathrm{sech}(t/\tau_0)]$. (b) Soliton regime, where there is a balance between nonlinearity and dispersion $[\Omega_{p1}(0,t)\tau_0 = 7\,\mathrm{sech}(t/\tau_0), \Omega_{p2}(0,t)\tau_0 = 9.3\,\mathrm{sech}(t/\tau_0)]$. (c) Nonlinearity-dominant regime $[\Omega_{p1}(0,t)\tau_0 = 9\,\mathrm{sech}(t/\tau_0), \Omega_{p2}(0,t)\tau_0 = 12\,\mathrm{sech}(t/\tau_0)]$. The lines from 1 to 6 in each panel correspond to propagation distance $z = 0$, 3 cm, 6 cm, 9 cm, 12 cm, and 15 cm, respectively. The control field $|\Omega_c\tau_0|$ is shown in the upper part of each panel.

all systems considered in those studies work in a linear propagation regime. Recently, in Refs. [3,4] a preliminary analysis has shown the possibility of realizing memory of a single-component optical soliton in three-level atomic systems via a single EIT. However, for light information processing (especially multibit applications) it is necessary to extend these studies not only to the nonlinear regime but also for multicomponent optical solitons. In this section, we demonstrate that it is possible to realize the storage and retrieval of the VOS by using the four-level tripod-type atomic system via DEIT.

To this aim, we consider the solution of the MB Eqs. (2) and (4) by using a particular control field that is adiabatically changed with time t to realize the function of its turning on and off. Since in this case analytical solutions of the MB equations are not available, we must resort to numerical simulations.

Figure 3 shows the result of a numerical simulation on the evolution of $|\Omega_{p1}\tau_0|$ (blue solid line) and $|\Omega_{p2}\tau_0|$ (red dashed line) as functions of z and t for different input light intensity of the probe pulse. In the simulation, the switching-on and the switching-off of the control field (the green solid line shown in the upper part of each panel) is modeled by the combination of two hyperbolic tangent functions with the form,

$$\Omega_c(0,t) = \Omega_{c0}\left\{1 - \frac{1}{2}\tanh\left[\frac{t - T_{\mathrm{off}}}{T_s}\right] + \frac{1}{2}\tanh\left[\frac{t - T_{\mathrm{on}}}{T_s}\right]\right\}, \tag{15}$$

where T_{off} and T_{on} are, respectively, the times of the switching-off and the switching-on with a switching time approximately given by T_s. Lines from 1 to 6 in the figure are for the pulse propagating to $z = 0$, 3 cm, 6 cm, 9 cm, 12 cm, and 15 cm, respectively. The system parameters are chosen from a typical cold alkali-metal ^{87}Rb atomic gas with $\Gamma_4/2\pi \approx 6$ MHz, $\Gamma_3/2\pi \approx 3.2$ kHz, $\gamma_{41}\tau_0 \approx \gamma_{42}\tau_0 \approx \gamma_{43}\tau_0 \approx 1.88$, $\gamma_{31}\tau_0 \approx \gamma_{32}\tau_0 \approx 10^{-4}$, $\Delta_2\tau_0 = 0.001$, $\Delta_3\tau_0 = 0.2$, $\Delta_4\tau_0 = 60$, $\kappa_{14}\tau_0 \approx \kappa_{24}\tau_0 = 1.5 \times 10^3$ cm^{-1}, $\Omega_{c0}\tau_0 = 24$, $T_s/\tau_0 = 0.2$, $T_{\mathrm{off}}/\tau_0 = 10$, $T_{\mathrm{on}}/\tau_0 = 20$, with $\tau_0 = 10^{-7}$s. Note that in order to plot clearly the profiles corresponding to different polarization components of the probe pulse, the peak values of $|\Omega_{p1}\tau_0|$ and $|\Omega_{p2}\tau_0|$ are taken to be different (as a special case, they can of course take the same value).

To describe the light pulse memory quantitatively, similar to Ref. [34] we define memory efficiency η_i as the probability of retrieving the ith component of the VOS after some storage time, or equivalently, as the energy ratio between the retrieved (output) pulse $\Omega_{pi}^{\text{output}}(t)$ and the input pulse $\Omega_{pi}^{\text{input}}(t)$:

$$\eta_i = \frac{\int_{-\infty}^{+\infty} \left|\Omega_{pi}^{\text{output}}(t)\right|^2 dt}{\int_{-\infty}^{+\infty} \left|\Omega_{pi}^{\text{input}}(t)\right|^2 dt}. \tag{16}$$

To characterize the quality of the generation of the pulse shape, we define an overlap integral J_i^2 as [35]

$$J_i^2 = \frac{\left|\int_{-\infty}^{+\infty} \Omega_{pi}^{\text{output}}(t)\Omega_{pi}^{\text{input}}(t+t_0)dt\right|^2}{\int_{-\infty}^{+\infty} \left|\Omega_{pi}^{\text{output}}(t)\right|^2 dt \cdot \int_{-\infty}^{+\infty} \left|\Omega_{pi}^{\text{input}}(t+t_0)\right|^2 dt}. \tag{17}$$

Line 1 and line 6 in the figure are taken as the input pulse $\Omega_{pi}^{\text{input}}(t)$ and output pulse $\Omega_{pi}^{\text{output}}(t)$ $(i = 1,2)$, respectively.

Shown in Fig. 3(a) is the result for a weak (i.e., linear) two-component probe pulse with $\Omega_{p1}(0,t)\tau_0 = 0.6\,\text{sech}(t/\tau_0)$ and $\Omega_{p2}(0,t)\tau_0 = 0.8\,\text{sech}(t/\tau_0)$. In this *dispersion-dominant regime*, storage and retrieval of the two-component probe pulse are possible, with the memory efficiencies for the two components of the probe pulse given by $\eta_1 \approx \eta_2 = 0.965$. The values of the overlap integral between the output and input pulses are $J_1^2 \approx J_2^2 = 0.658$. Thus the fidelity of the light memory is only $\eta_1 J_1^2 \approx \eta_2 J_2^2 = 0.635$, which means that a large deformation for the retrieved pulse shape occurs and both components of the probe fields broaden rapidly before and after the storage. Obviously, such light memory is not desirable for practical application because light information will be spoiled after the storage.

Figure 3(b) shows the result for a weak nonlinear two-component probe pulse with $\Omega_{p1}(0,t)\tau_0 = 7\,\text{sech}(t/\tau_0)$ and $\Omega_{p2}(0,t)\tau_0 = 9.3\,\text{sech}(t/\tau_0)$. In this case, the system works in a *soliton regime* where a balance between dispersion and nonlinearity is achieved. Before the storage (Ω_c is switched on), the probe pulse is a VOS with two components, i.e., a soliton pair; when Ω_c is switched off, the VOS is stored in the atomic ensemble (i.e., both Ω_{p1} and Ω_{p2} are vanishing but the atomic coherences σ_{13} and σ_{23} take nonzero values; see below); then the VOS is retrieved after the storage (when Ω_c is switched on again). The memory efficiencies for the two components of the probe pulse are $\eta_1 \approx \eta_2 = 0.961$. The values of the overlap integral between the output and input pulses is $J_1^2 \approx J_2^2 = 0.932$ and the fidelity of the retrieved pulse is $\eta_1 J_1^2 \approx \eta_2 J_2^2 = 0.896$. We see that the retrieved probe pulse has nearly the same wave shape as that before the storage and hence the light memory in this case has high efficiency and fidelity. This result illustrates clearly that a robust memory of the VOS can be realized in the present four-level tripod system via the DEIT.

Shown in Fig. 3(c) is the result for the case of strong nonlinearity with $\Omega_{p1}(0,t)\tau_0 = 9\,\text{sech}(t/\tau_0)$ and $\Omega_{p2}(0,t)\tau_0 = 12\,\text{sech}(t/\tau_0)$. In this case, the system works in a *nonlinearity-dominant regime* and hence a stable VOS is not possible. From the figure we see indeed that both components of the probe pulse display significant distortions; especially some new peaks are generated before and after the storage. The memory efficiencies for the two components of the probe pulse are $\eta_1 \approx \eta_2 = 0.942$. The values of the overlap integral between the output and input pulses are $J_1^2 \approx J_2^2 = 0.731$ and hence the fidelity of the retrieved pulse is only $\eta_1 J_1^2 \approx \eta_2 J_2^2 = 0.689$. Thus, similar to the dispersion-dominant regime [i.e., Fig. 3(a)], the light memory in this situation has a low fidelity, which is also not desirable for practical application because light information will be lost before and after the storage.

B. Behavior of the atomic coherences σ_{13} and σ_{23} and the dynamics of the control field during the light memory

From the result of Fig. 3, we clearly see that comparing with the dispersion-dominant and nonlinearity-dominant regimes the soliton regime is desirable for the storage and retrieval of the two components of the probe pulse (i.e., VOS). One may ask the question how the VOS is stored into the atomic ensemble when both the probe and control fields have vanishing value. In fact, during the storage the probe-field energy is converted into atomic degrees of freedom, i.e., into the atomic coherence σ_{13} and σ_{23}, which have nonvanishing values even when Ω_c, Ω_{p1}, and Ω_{p2} become zero (see the theoretical explanation given below).

Illustrated in Fig. 4 is the result of atomic coherences σ_{13} (blue solid line) and σ_{23} (red dashed line) for the three different dynamic regimes as functions of distance z and time t during the process of the storage and retrieval of the two-component probe pulse. The initial probe pulse used in the dispersion-dominant regime [Fig. 4(a)], the soliton regime [Fig. 4(b)], and the nonlinearity-dominant regime [Fig. 4(c)] are the same as those used in Figs. 3(a)–3(c), respectively. The lines from 1 to 6 in each panel of the figure correspond to $z = 0$, 3 cm, 6 cm, 9 cm, 12 cm, and 15 cm, respectively.

From Fig. 4 combined with Fig. 3 we see that, during the storage and retrieval of the probe pulse, $\sigma_{13} \neq 0$ and $\sigma_{23} \neq 0$ in the time interval when $\Omega_c = \Omega_{p1} = \Omega_{p2} = 0$. Since the two components of the probe pulse are stored in the form of atomic coherences when the control field is switched off and is retained until the control field is switched on again, the atomic coherences σ_{13} and σ_{23} can be taken as the intermediaries for the storage and retrieval of the two components of the probe pulse.

Note that in the above discussions on the memory of the probe pulse, the dynamics of the control field is disregarded. However, because in the interval of the storage the control field becomes vanishingly small and its depletion (dynamics) is an important issue. Shown in Fig. 5 is the result for the depletion of the control field during the storage and retrieval of the VOS. Figure 5(a) shows the evolution of $|\Omega_{p1}\tau_0|$ (blue solid line), $|\Omega_{p2}\tau_0|$ (red dashed line), and $|\Omega_c\tau_0|$ (green solid line) as functions of t and z in the soliton regime. Figure 5(b) shows the corresponding atomic coherences σ_{13} and σ_{23} as functions of z and t. The lines from 1 to 6 in each panel correspond to $z = 0$, 2 cm, 4 cm, 6 cm, 8 cm, and 10 cm, respectively. From the figure we see that, as expected, the control field $|\Omega_c\tau_0|$ has indeed small depletion before and after the storage of the VOS.

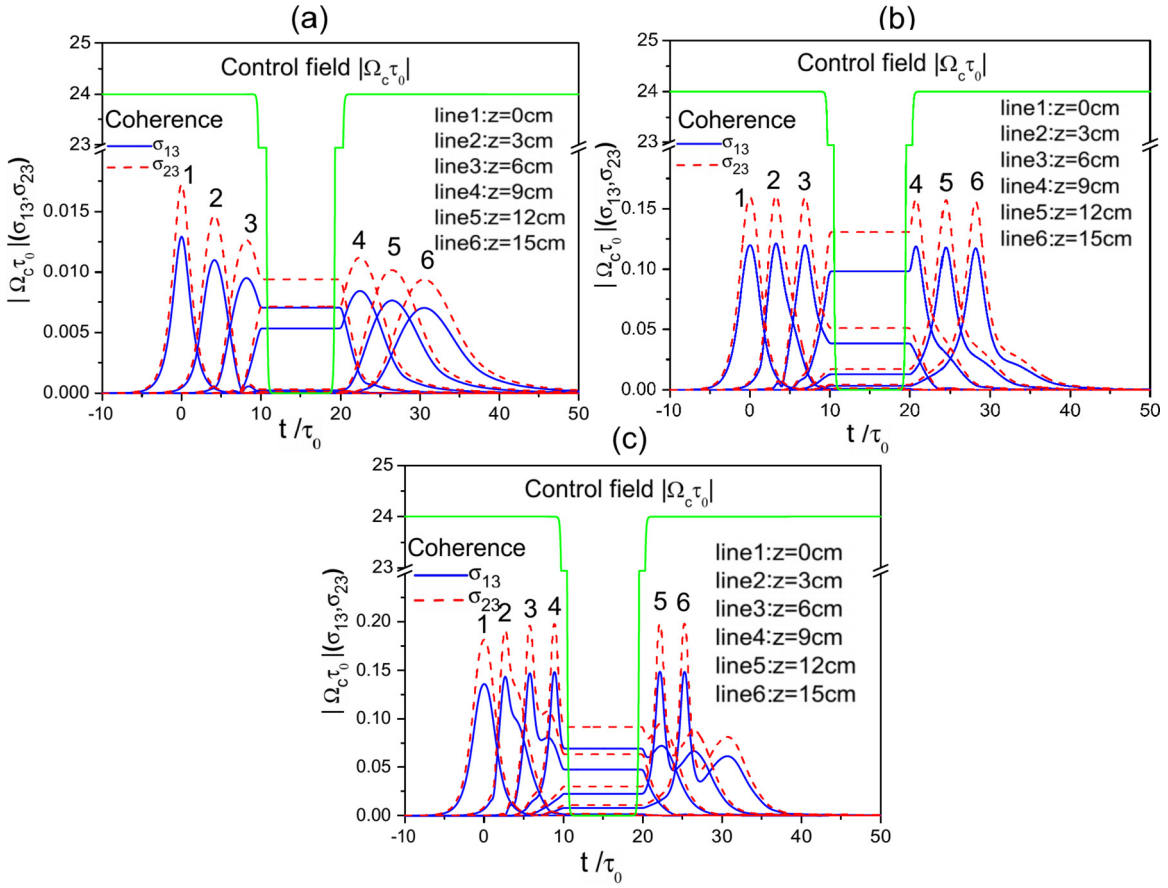

FIG. 4. (Color online) Atomic coherences σ_{13} (blue solid line) and σ_{23} (red dashed line) in the three different dynamic regimes as functions of distance z and time t during the process of the storage and retrieval of the two-component probe pulse. Initial probe pulse used in the dispersion-dominant regime (a), the soliton regime (b), and the nonlinearity-dominant regime (c) are the same as those used in Figs. 3(a)–3(c), respectively. The lines from 1 to 6 in each panel correspond to $z = 0$, 3 cm, 6 cm, 9 cm, 12 cm, and 15 cm, respectively.

C. Theoretical explanation

Now we give a simple explanation on the numerical results of the VOS memory presented above, paying attention mainly to Figs. 3(b), 4(b), and 5(a).

Because before and after the storage the leading order of Ω_c is a constant, the theoretical approach presented in Sec. III is valid. During the storage, Ω_c is switching off and the two components of the VOS become nearly vanishing. Thus in the

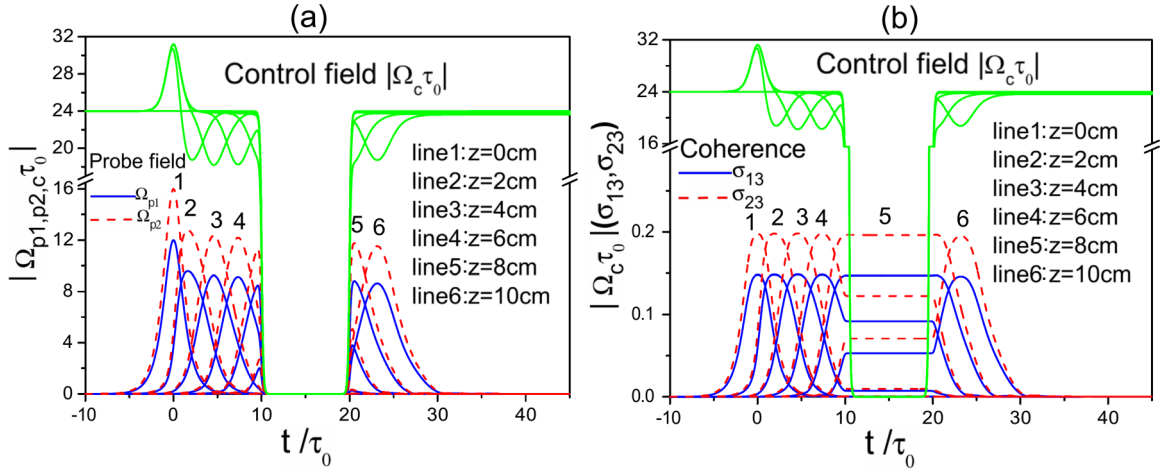

FIG. 5. (Color online) Depletion of the control field during the storage and retrieval of the VOS. (a) Evolution of $|\Omega_{p1}\tau_0|$ (blue solid line), $|\Omega_{p2}\tau_0|$ (red dashed line), and $|\Omega_c\tau_0|$ (green solid line) as functions of t and z in the soliton regime. (b) Corresponding atomic coherences σ_{13} and σ_{23} as functions of z and t. The lines from 1 to 6 in each panel correspond to $z = 0$, 2 cm, 4 cm, 6 cm, 8 cm, and 10 cm, respectively.

soliton regime the probe pulse can be written as the form,

$$\Omega_{p1}(z,t) \approx \begin{cases} \frac{1}{\tau_0}\sqrt{\left|\frac{\tilde{W}_{12}\tilde{K}_{22}}{\tilde{W}_{11}\tilde{W}_{22}}\right|}\,\mathrm{sech}\left[\frac{A_0}{\tau_0}\left(t-\frac{z}{\tilde{V}_g}\right)+\frac{B_0 z}{L_D}\right]e^{i\phi_1}, & \text{for} \quad t < \mathrm{T_{off}}, \\ 0, & \text{for} \quad \mathrm{T_{off}} \leqslant t \leqslant \mathrm{T_{on}}, \\ \frac{1}{\tau_0}\sqrt{\left|\frac{\tilde{W}_{12}\tilde{K}_{22}}{\tilde{W}_{11}\tilde{W}_{22}}\right|}\,\mathrm{sech}\left[\frac{A_0}{\tau_0}\left(t-\frac{z}{\tilde{V}_g}\right)+\frac{B_0 z}{L_D}\right]e^{i(\phi_1+\phi_0)}, & \text{for} \quad t > \mathrm{T_{on}}, \end{cases} \tag{18}$$

$$\Omega_{p2}(z,t) \approx \begin{cases} \frac{1}{\tau_0}\sqrt{\left|\frac{A_0^2\tilde{K}_{12}\tilde{W}_{22}}{\tilde{W}_{12}\tilde{K}_{22}}\right|-1}\sqrt{\left|\frac{\tilde{K}_{22}}{\tilde{W}_{22}}\right|}\,\mathrm{sech}\left[\frac{A_0}{\tau_0}\left(t-\frac{z}{\tilde{V}_g}\right)+\frac{B_0 z}{L_D}\right]e^{i\phi_2}, & \text{for} \quad t < \mathrm{T_{off}}, \\ 0, & \text{for} \quad \mathrm{T_{off}} \leqslant t \leqslant \mathrm{T_{on}}, \\ \frac{1}{\tau_0}\sqrt{\left|\frac{A_0^2\tilde{K}_{12}\tilde{W}_{22}}{\tilde{W}_{12}\tilde{K}_{22}}\right|-1}\sqrt{\left|\frac{\tilde{K}_{22}}{\tilde{W}_{22}}\right|}\,\mathrm{sech}\left[\frac{A_0}{\tau_0}\left(t-\frac{z}{\tilde{V}_g}\right)+\frac{B_0 z}{L_D}\right]e^{i(\phi_2+\phi_0)}, & \text{for} \quad t > \mathrm{T_{on}}, \end{cases} \tag{19}$$

where $\phi_1 = \tilde{K}_1 z + B_0|\tilde{K}_{22}|(t - z/\tilde{V}_g)/(A_0\tilde{K}_{12}\tau_0) - (z/L_D)(A_0^4\tilde{K}_{12}^2 - B_0^2\tilde{K}_{22}^2)/(2A_0^2|\tilde{K}_{22}|\tilde{K}_{12})$, $\phi_2 = \tilde{K}_2 z + B_0(t - z/\tilde{V}_g)/(A_0\tau_0) - (z/L_D)(A_0^4 - B_0^2)/(2A_0^2)$, ϕ_0 is a constant phase factor and A_0, B_0 are also free parameters. Thus the result numerically found in Fig. 3(b) can be well explained.

The behavior observed numerically in Fig. 4(b) can be understood as follows. Before and after the storage of the VOS, the theoretical approach presented in Sec. III can be used. By the result given by Eqs. (C1a) and (C1c), we have $\sigma_{13} \sim \Omega_{p1}^*$ and $\sigma_{23} \sim \Omega_{p2}^*$. Thus before and after the storage both σ_{13} and σ_{23} have forms similar to solitons because Ω_{p1}^* and Ω_{p2}^* are the components of the VOS.

However, in the interval of the storage of the VOS, the behavior of σ_{13} and σ_{23} cannot be explained by using the perturbation theory developed in Sec. III because in this interval Ω_c is a small quantity. To solve this problem, we turn to consider the Bloch Eq. (2) directly. Since $d_{31}\sigma_{31}$, $d_{32}\sigma_{32}$, $\Omega_{p1}\sigma_{43}^*$, and $\Omega_{p2}\sigma_{43}^*$ are small, by Eqs. (A1f) and (A1g) we obtain

$$\sigma_{41} \approx -\frac{i}{\Omega_c^*}\frac{\partial\sigma_{31}}{\partial t}, \tag{20a}$$

$$\sigma_{42} \approx -\frac{i}{\Omega_c^*}\frac{\partial\sigma_{32}}{\partial t}. \tag{20b}$$

In addition, by Eqs. (A1h) and (A1i) we have

$$\sigma_{31} \approx -\frac{\Omega_{p1}}{2\Omega_c} - \frac{1}{\Omega_c}\left(i\frac{\partial}{\partial t} + d_{41}\right)\sigma_{41}, \tag{21a}$$

$$\sigma_{32} \approx -\frac{\Omega_{p2}}{2\Omega_c} - \frac{1}{\Omega_c}\left(i\frac{\partial}{\partial t} + d_{42}\right)\sigma_{42}. \tag{21b}$$

Substituting Eq. (20) into Eq. (21) we obtain

$$\begin{aligned}\sigma_{13} &= -\frac{1}{2}\left(\frac{\Omega_{p1}}{\Omega_c}\right)^* - \frac{1}{|\Omega_c|^2}\left(\frac{\partial}{\partial t} + id_{41}^*\right)\frac{\partial\sigma_{13}}{\partial t} \\ &\approx -\frac{1}{2}\left(\frac{\Omega_{p1}}{\Omega_c}\right)^*, \end{aligned} \tag{22a}$$

$$\begin{aligned}\sigma_{23} &= -\frac{1}{2}\left(\frac{\Omega_{p2}}{\Omega_c}\right)^* - \frac{1}{|\Omega_c|^2}\left(\frac{\partial}{\partial t} + id_{42}^*\right)\frac{\partial\sigma_{23}}{\partial t} \\ &\approx -\frac{1}{2}\left(\frac{\Omega_{p2}}{\Omega_c}\right)^*. \end{aligned} \tag{22b}$$

Consequently, σ_{13} and σ_{23} are nonzero if the ratios Ω_{p1}/Ω_c and Ω_{p2}/Ω_c can keep finite values. This can be realized by adiabatically decreasing Ω_c, by which the values of Ω_{p1} and Ω_{p2} also become zero with the same rate during the storage.

One can also understand this point from the viewpoint of dark states. Since our tripod system has two dark states (7a) and (7b), it starts from these two dark states in the optical excitation. Notice that the dark states (7a) and (7b) can be written as the form,

$$|D_1\rangle = \Omega_c[|1\rangle - (\Omega_{p1}/\Omega_c)|3\rangle], \tag{23a}$$

$$|D_2\rangle = \Omega_c[|2\rangle - (\Omega_{p2}/\Omega_c)|3\rangle], \tag{23b}$$

thus the system can keep in these two dark states when σ_{13} and σ_{23} have nonzero values during the storage.

We now turn to consider Fig. 5(a). Since the control field has small depletion before and after the storage of the VOS, we solve Eq. (4c) by using the perturbation expansion,

$$\Omega_c = \Omega_c^{(0)} + \epsilon\Omega_c^{(1)} + \epsilon^2\Omega_c^{(2)} + \cdots, \tag{24}$$

which is valid for the time interval before and after the VOS storage where the leading order of Ω_c (i.e., $\Omega_c^{(0)}$) has a large value. Substituting the expansion (24) into Eq. (4c) and solving the equations for $\Omega_c^{(l)}$ ($l = 0,1,2,...$), we obtain the following conclusions: (i) $\Omega_c^{(0)}$ is a constant, which corresponds to the horizontal line in the upper part of Fig. 5(a). (ii) $\Omega_c^{(1)}(t,z) = \Omega_c^{(1)}(t - z/c)$ describes a small hump close to the (green solid) horizontal line on the upper part of the figure, which propagates with velocity c. The concrete form of $\Omega_c^{(1)}$ relies on the initial condition. (iii) $\Omega_c^{(2)}$ satisfies the equation $i\partial\Omega_c^{(2)}/\partial z = -\kappa_{34}\sigma_{43}^{(2)}$. We obtain

$$\Omega_c^{(2)} \approx -i\kappa_{34}\frac{\tilde{V}_g}{\tau_0}\frac{\tilde{K}_{22}}{\tilde{W}_{22}}\left(a_{431}^{(2)} + a_{432}^{(2)}\right)\tanh\left[\frac{1}{\tau_0}\left(t - \frac{z}{\tilde{V}_g}\right)\right], \tag{25}$$

which contributes a hole to the horizontal (green solid) line on the upper part of Fig. 5(a). Physically, the appearance of the control-field depletion is due to the energy exchange between the control field and the probe field via the atomic ensemble as an intermediary.

V. STORAGE AND RETRIEVAL OF N-COMPONENT OPTICAL SOLITONS

The theoretical approach presented above can be generalized to a $(N+1)$-pod system with N independent probe pulses ($N > 2$). Figure 6(a) shows the energy-level diagram and excitation scheme of a $(N+1)$-pod atomic system [38]. The N probe pulses (with half-Rabi frequencies $\Omega_{p1}, \Omega_{p2}, \ldots,$

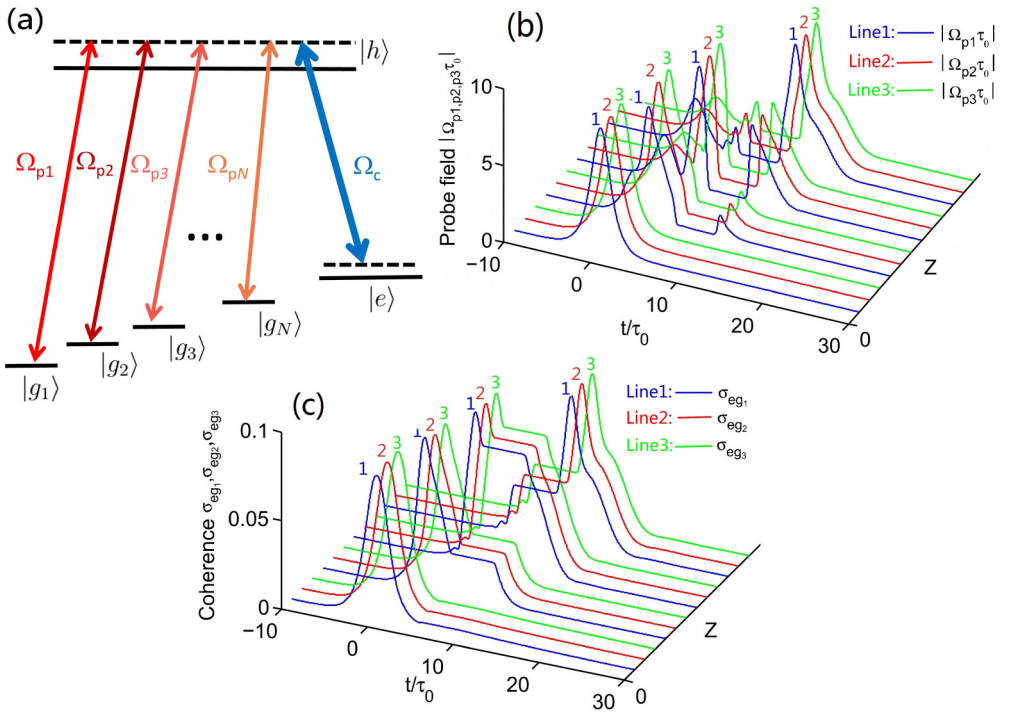

FIG. 6. (Color online) (a) Energy-level diagram and excitation scheme of the $(N+1)$-pod atomic system. The N probe pulses drive, respectively, the transitions from $|g_1\rangle \leftrightarrow |h\rangle$, $|g_2\rangle \leftrightarrow |h\rangle$, $|g_3\rangle \leftrightarrow |h\rangle, \ldots,$ and $|g_N\rangle \leftrightarrow |h\rangle$; one continuous-wave control field drives the transitions from $|h\rangle \leftrightarrow |e\rangle$. (b) Storage and retrieval of three-component optical soliton in the quadric-pod system. Evolution of $|\Omega_{p1}\tau_0|$ (blue line), $|\Omega_{p2}\tau_0|$ (red line), and $|\Omega_{p3}\tau_0|$ (green line) as functions of z and t, with $\Omega_{pl}(0,t) = 8\,\mathrm{sech}(t/\tau_0)$ $(l = 1,2,3)$. (c) The atomic coherences σ_{eg_1} (blue line), σ_{eg_2} (red line), and σ_{eg_3} (green line) as functions of distance z and t during the storage and retrieval of the three-component optical soliton.

and Ω_{pN}) drive, respectively, the transitions from $|g_1\rangle \leftrightarrow |h\rangle$, $|g_2\rangle \leftrightarrow |h\rangle, |g_3\rangle \leftrightarrow |h\rangle, \ldots,$ and $|g_N\rangle \leftrightarrow |h\rangle$; one continuous-wave control field (with half-Rabi frequency Ω_c) drives the transitions from $|h\rangle \leftrightarrow |e\rangle$. One can obtain N dark states and N branches of linear dispersion relation, and hence the system allows N electromagnetically induced transparency (NEIT). Based on the NEIT one can derive N coupled NLS equations and found N coupled soliton solutions, and then discuss the storage and retrieval of the N-component optical soliton.

For simplicity, we consider here a quadri-pod system $(N = 3)$. Following a similar procedure developed in Sec. III, we can obtain three dark states and three branches of the linear dispersion relation of the system. It is easy to show that the system admits triple electromagnetically induced transparency (TEIT) when the control field is strong. That is to say, when the TEIT occurs each of $\mathrm{Im}(K_j)$ $(j = 1,2,3)$ opens an EIT transparency window at almost the same position. Additionally, the envelopes of the three probe pulses travel with ultraslow group velocities which are matched well due to the symmetry of the system.

We can also derive the equations for the envelopes F_l of the half-Rabi frequencies Ω_{pl} $(l = 1,2,3)$ by using the method of multiple scales. The result reads

$$i\frac{\partial F_1}{\partial z_2} - \frac{1}{2}K_{12}\frac{\partial^2 F_1}{\partial t_1^2} - (W_{11}|F_1|^2 e^{-2\bar{\alpha}_1 z_2} + W_{12}|F_2|^2 e^{-2\bar{\alpha}_2 z_2} + W_{13}|F_3|^2 e^{-2\bar{\alpha}_3 z_2})F_1 = 0,$$

$$i\frac{\partial F_2}{\partial z_2} - \frac{1}{2}K_{22}\frac{\partial^2 F_2}{\partial t_1^2} - (W_{21}|F_1|^2 e^{-2\bar{\alpha}_1 z_2} + W_{22}|F_2|^2 e^{-2\bar{\alpha}_2 z_2} + W_{23}|F_3|^2 e^{-2\bar{\alpha}_3 z_2})F_2 = 0,$$

$$i\frac{\partial F_3}{\partial z_2} - \frac{1}{2}K_{32}\frac{\partial^2 F_3}{\partial t_1^2} - (W_{31}|F_1|^2 e^{-2\bar{\alpha}_1 z_2} + W_{32}|F_2|^2 e^{-2\bar{\alpha}_2 z_2} + W_{33}|F_3|^2 e^{-2\bar{\alpha}_3 z_2})F_3 = 0,$$

where $K_{l2} = \partial^2 K_l/\omega^2, \bar{\alpha}_l = \epsilon^{-2}\mathrm{Im}(K_l)$ $(l = 1,2,3)$, W_{ll} $(W_{jl}$; $j \neq l)$ are SPM (CPM) coefficients. Their explicit expressions are omitted here. We stress that in order to have a significant interaction between different components the detunings for all the lower levels should be taken small.

At TEIT condition, imaginary parts of the coefficients in the above envelope equations are small compared with their real parts. Thus at leading order these equations can be reduced to three coupled NLS equations and a three-component soliton solution can be obtained analytically [36]. All components in such soliton have nearly the same, ultraslow propagating velocity and ultralow generation power. Due to the existence of the three dark states, they can also be stored and retrieved by adiabatically manipulating the control field.

Figure 6(b) shows the evolution of $|\Omega_{p1}\tau_0|$ (blue line), $|\Omega_{p2}\tau_0|$ (red line), and $|\Omega_{p3}\tau_0|$ (green line) as functions of the distance z and time t, with $\Omega_{pl}(0,t) = 8\,\mathrm{sech}(t/\tau_0)$ $(l = 1,2,3)$. The system parameters have been chosen to work in the soliton regime with a balance between dispersion and

nonlinearity. We see that all $|\Omega_{pl}\tau_0|$ ($l = 1,2,3$) evolve first into a solitonlike pulse before the storage; later on they are stored in the atomic ensemble with Ω_{pl} ($l = 1,2,3$) when Ω_c is switched off; then they are retrieved when Ω_c is switched on. The retrieved pulses have nearly the same wave shapes as those before the storage. We see that it is indeed possible to realize a robust memory of three-component optical solitons in the system.

Figure 6(c) shows the result of the atomic coherences σ_{eg_1} (blue line), σ_{eg_2} (red line), and σ_{eg_3} (green line) as functions of z and t. We see that the atomic coherences have nonzero values during the storage of the three-component optical soliton. A similar theoretical explanation on these numerical results presented here can also be given as done in Sec. IV C.

Note that for the storage and retrieval of the N-component optical pulses one cannot assign N components with different polarizations by using a single probe field. The reason is that a single probe field has only two independent polarizations (which can be used to realize the vector optical solitons and their storage and retrieval as analyzed in Secs. III and IV). In general, for the $(N+1)$-pod system one can choose N different probe fields having different polarizations, as considered in Refs. [38,39].

VI. SUMMARY

We have proposed a scheme to realize storage and retrieval of two-component optical solitons in a coherent atomic system. The system we have considered is a cold, lifetime broadened four-level atomic gas with a tripod configuration working at the condition of DEIT. We have shown that due to the existence of the two dark states, the optical absorption of the probe pulse can be largely reduced. In addition, the two orthogonal polarization components of the probe pulse with a form of VOS cannot only be slowed down substantially but also be stored and retrieved robustly by switching a control laser field off and on. We have also shown that it is possible to achieve a memory of the N-component optical soliton by using the N dark states in a $(N+1)$-pod system ($N > 2$). The results reported here may have promise in applications for high-fidelity light information processing in a weak nonlinear regime.

ACKNOWLEDGMENT

This work was supported by the NSF-China under Grants No. 11475063, No. 11174080, No. 11474099, and No. 11475063.

APPENDIX A: DETAILED EXPRESSION OF THE BLOCH EQUATION

Under electric-dipole and rotating-wave approximations, the equations of the motion for the density matrix elements σ_{jl} in the interaction picture are

$$i\left(\frac{\partial}{\partial t}+\Gamma_{31}\right)\sigma_{11}-i(\Gamma_{13}\sigma_{33}+\Gamma_{14}\sigma_{44})+\Omega_{p1}^{*}\sigma_{41}-\Omega_{p1}\sigma_{41}^{*}=0, \tag{A1a}$$

$$i\left(\frac{\partial}{\partial t}+\Gamma_{32}\right)\sigma_{22}-i(\Gamma_{23}\sigma_{33}+\Gamma_{24}\sigma_{44})+\Omega_{p2}^{*}\sigma_{42}-\Omega_{p2}\sigma_{42}^{*}=0, \tag{A1b}$$

$$i\left(\frac{\partial}{\partial t}+\Gamma_{3}\right)\sigma_{33}-i\Gamma_{31}\sigma_{11}-i\Gamma_{32}\sigma_{22}-i\Gamma_{34}\sigma_{44}+\Omega_{c}^{*}\sigma_{43}-\Omega_{c}\sigma_{43}^{*}=0, \tag{A1c}$$

$$i\left(\frac{\partial}{\partial t}+\Gamma_{4}\right)\sigma_{44}+\Omega_{p1}\sigma_{41}^{*}+\Omega_{p2}\sigma_{42}^{*}+\Omega_{c}\sigma_{43}^{*}-\Omega_{p1}^{*}\sigma_{41}-\Omega_{p2}^{*}\sigma_{42}-\Omega_{c}^{*}\sigma_{43}=0, \tag{A1d}$$

$$\left(i\frac{\partial}{\partial t}+d_{21}\right)\sigma_{21}+\Omega_{p2}^{*}\sigma_{41}-\Omega_{p1}\sigma_{42}^{*}=0, \tag{A1e}$$

$$\left(i\frac{\partial}{\partial t}+d_{31}\right)\sigma_{31}+\Omega_{c}^{*}\sigma_{41}-\Omega_{p1}\sigma_{43}^{*}=0, \tag{A1f}$$

$$\left(i\frac{\partial}{\partial t}+d_{32}\right)\sigma_{32}+\Omega_{c}^{*}\sigma_{42}-\Omega_{p2}\sigma_{43}^{*}=0, \tag{A1g}$$

$$\left(i\frac{\partial}{\partial t}+d_{41}\right)\sigma_{41}+\Omega_{p1}(\sigma_{11}-\sigma_{44})+\Omega_{p2}\sigma_{21}+\Omega_{c}\sigma_{31}=0, \tag{A1h}$$

$$\left(i\frac{\partial}{\partial t}+d_{42}\right)\sigma_{42}+\Omega_{p2}(\sigma_{22}-\sigma_{44})+\Omega_{p1}\sigma_{21}^{*}+\Omega_{c}\sigma_{32}=0, \tag{A1i}$$

$$\left(i\frac{\partial}{\partial t}+d_{43}\right)\sigma_{43}+\Omega_{c}(\sigma_{33}-\sigma_{44})+\Omega_{p1}\sigma_{31}^{*}+\Omega_{p2}\sigma_{32}^{*}=0, \tag{A1j}$$

where $\Omega_{p1}=(\hat{\epsilon}_{-}\cdot\mathbf{p}_{14})\mathcal{E}_{p^{-}}/\hbar$ ($\Omega_{p2}=(\hat{\epsilon}_{+}\cdot\mathbf{p}_{24})\mathcal{E}_{p^{+}}/\hbar$) is the half-Rabi frequency of the $\mathcal{E}_{p^{-}}$ ($\mathcal{E}_{p^{+}}$) component of the probe field; $\Omega_c=(\hat{\epsilon}_c\cdot\mathbf{p}_{34})\mathcal{E}_c/\hbar$ is the half-Rabi frequency of the control field, with $\mathbf{p}_{ij}$ the electric dipole matrix element associated with the transition between $|j\rangle$ and $|i\rangle$; $d_{jl}=\Delta_j-\Delta_l+i\gamma_{jl}$, with the population decay rates and coherence decay rates defined, respectively, by $\Gamma_j=\sum_{i<j}\Gamma_{ij}$ and $\gamma_{ij}=(\Gamma_i+\Gamma_j)/2+\gamma_{ij}^{\mathrm{col}}$. Γ_{14}, Γ_{24}, and Γ_{34} are, respectively, the spontaneous emission

decay rate from $|4\rangle$ to $|1\rangle$, $|4\rangle$ to $|2\rangle$, and $|4\rangle$ to $|3\rangle$. Γ_{13}, Γ_{31}, Γ_{23}, and Γ_{32} are, respectively, the rates of incoherent population transfer between $|3\rangle$ and $|1\rangle$, and between $|3\rangle$ and $|2\rangle$ [16].

The model given above can be easily realized by selecting realistic physical systems. One of them is the D2 line of ^{87}Rb atomic gas with the energy levels selected as [37]

$$|1\rangle = |5^2S_{1/2}, F = 1, m_F = 1\rangle, \quad |2\rangle = |5^2S_{1/2}, F = 1, m_F = -1\rangle, \tag{A2}$$

$$|3\rangle = |5^2S_{1/2}, F = 2, m_F = 0\rangle, \quad |4\rangle = |5^2P_{3/2}, F = 2, m_F = 0\rangle,$$
$$\Gamma_4/2\pi \approx 6.06 \text{ MHz}, \quad \Gamma_3/2\pi = 3200 \text{ Hz},$$
$$\gamma_{41} \approx \gamma_{42} \approx \gamma_{43} \approx 18.8 \text{ MHz}, \quad \gamma_{31} \approx \gamma_{32} \approx 1000 \text{ Hz}. \tag{A3}$$

APPENDIX B: EXPRESSIONS OF THE COEFFICIENTS IN EQ. (5)

$$X_1 = i(\Gamma_3 + \Gamma_{31}) + |\Omega_c|^2\left(\frac{1}{d_{43}} - \frac{1}{d_{43}^*}\right), \tag{B1a}$$

$$X_2 = i(\Gamma_3 + \Gamma_{32}) + |\Omega_c|^2\left(\frac{1}{d_{43}} - \frac{1}{d_{43}^*}\right), \tag{B1b}$$

$$X_4 = i(\Gamma_3 + \Gamma_{34}) + 2|\Omega_c|^2\left(\frac{1}{d_{43}} - \frac{1}{d_{43}^*}\right), \tag{B1c}$$

$$G_1 = i\Gamma_{13} + \frac{\Gamma_{13} - \Gamma_{14}}{X_4}\left[\Gamma_3 + i|\Omega_c|^2\left(\frac{1}{d_{43}} - \frac{1}{d_{43}^*}\right)\right], \tag{B1d}$$

$$G_2 = i\Gamma_{23} + \frac{\Gamma_{23} - \Gamma_{24}}{X_4}\left[\Gamma_3 + i|\Omega_c|^2\left(\frac{1}{d_{43}} - \frac{1}{d_{43}^*}\right)\right], \tag{B1e}$$

$$J_{11} = i(\Gamma_{31} + \Gamma_{13}) - \frac{i(\Gamma_{13} - \Gamma_{14})X_1}{X_4}, \tag{B1f}$$

$$J_{12} = i\Gamma_{13} - \frac{i(\Gamma_{13} - \Gamma_{14})X_2}{X_4}, \tag{B1g}$$

$$J_{21} = i\Gamma_{23} - \frac{i(\Gamma_{23} - \Gamma_{24})X_1}{X_4}, \tag{B1h}$$

$$J_{22} = i(\Gamma_{32} + \Gamma_{23}) - \frac{i(\Gamma_{23} - \Gamma_{24})X_2}{X_4}. \tag{B1i}$$

APPENDIX C: THE FIRST-ORDER SOLUTION

$$\sigma_{31}^{(1)} = -\frac{\Omega_c^*\left(\sigma_{11}^{(0)} - \sigma_{44}^{(0)}\right) + (\omega + d_{41})\sigma_{43}^{*(0)}}{D_1}F_1e^{i\theta_1}, \tag{C1a}$$

$$\sigma_{41}^{(1)} = \frac{(\omega + d_{31})\left(\sigma_{11}^{(0)} - \sigma_{44}^{(0)}\right) + \Omega_c\sigma_{43}^{*(0)}}{D_1}F_1e^{i\theta_1}, \tag{C1b}$$

$$\sigma_{32}^{(1)} = -\frac{\Omega_c^*\left(\sigma_{22}^{(0)} - \sigma_{44}^{(0)}\right) + (\omega + d_{42})\sigma_{43}^{*(0)}}{D_2}F_2e^{i\theta_2}, \tag{C1c}$$

$$\sigma_{42}^{(1)} = \frac{(\omega + d_{32})\left(\sigma_{22}^{(0)} - \sigma_{44}^{(0)}\right) + \Omega_c\sigma_{43}^{*(0)}}{D_2}F_2e^{i\theta_2}, \tag{C1d}$$

with other $\sigma_{jl}^{(1)} = 0$.

APPENDIX D: THE SECOND-ORDER SOLUTION

$$\sigma_{21}^{(2)} = \frac{1}{\omega + d_{21}}\left(\sigma_{42}^{*(1)}F_1e^{i\theta_1} - \sigma_{41}^{(1)}F_2^*e^{-i\theta_2^*}\right), \tag{D1a}$$

$$\sigma_{31}^{(2)} = \frac{i\left[\Omega_c^*a_{41}^{(1)} - (\omega + d_{41})a_{31}^{(1)}\right]}{D_1}\frac{\partial}{\partial t_1}F_1e^{i\theta_1}, \tag{D1b}$$

$$\sigma_{41}^{(2)} = \frac{i\left[\Omega_ca_{31}^{(1)} - (\omega + d_{31})a_{41}^{(1)}\right]}{D_1}\frac{\partial}{\partial t_1}F_1e^{i\theta_1}, \tag{D1c}$$

$$\sigma_{32}^{(2)} = \frac{i\left[\Omega_c^*a_{42}^{(1)} - (\omega + d_{42})a_{32}^{(1)}\right]}{D_2}\frac{\partial}{\partial t_1}F_2e^{i\theta_2}, \tag{D1d}$$

$$\sigma_{42}^{(2)} = \frac{i\left[\Omega_ca_{32}^{(1)} - (\omega + d_{32})a_{42}^{(1)}\right]}{D_2}\frac{\partial}{\partial t_1}F_2e^{i\theta_2}, \tag{D1e}$$

$$\sigma_{11}^{(2)} = a_{111}^{(2)}|F_1|^2e^{-2\bar{\alpha}_1z_2} + a_{112}^{(2)}|F_2|^2e^{-2\bar{\alpha}_2z_2}, \tag{D1f}$$

$$\sigma_{22}^{(2)} = a_{221}^{(2)}|F_1|^2e^{-2\bar{\alpha}_1z_2} + a_{222}^{(2)}|F_2|^2e^{-2\bar{\alpha}_2z_2}, \tag{D1g}$$

$$\sigma_{44}^{(2)} = a_{441}^{(2)}|F_1|^2e^{-2\bar{\alpha}_1z_2} + a_{442}^{(2)}|F_2|^2e^{-2\bar{\alpha}_2z_2}, \tag{D1h}$$

$$\sigma_{43}^{(2)} = a_{431}^{(2)}|F_1|^2e^{-2\bar{\alpha}_1z_2} + a_{432}^{(2)}|F_2|^2e^{-2\bar{\alpha}_2z_2}, \tag{D1i}$$

with

$$a_{111}^{(2)} = \frac{J_{12}C_1\frac{i(\Gamma_{23} - \Gamma_{24})}{X_4} - J_{22}\left[\frac{i(\Gamma_{13} - \Gamma_{14})}{X_4}C_1 - A_1\right]}{J_{21}J_{12} - J_{11}J_{22}},$$

$$a_{112}^{(2)} = \frac{J_{12}\left[\frac{i(\Gamma_{23} - \Gamma_{24})}{X_4}C_2 - B_2\right] - J_{22}C_2\frac{i(\Gamma_{13} - \Gamma_{14})}{X_4}}{J_{21}J_{12} - J_{11}J_{22}},$$

$$a_{221}^{(2)} = \frac{J_{21}\left[\frac{i(\Gamma_{13} - \Gamma_{14})}{X_4}C_1 - A_1\right] - J_{11}C_1\frac{i(\Gamma_{23} - \Gamma_{24})}{X_4}}{J_{21}J_{12} - J_{11}J_{22}},$$

$$a_{222}^{(2)} = \frac{J_{21}C_2\frac{i(\Gamma_{13} - \Gamma_{14})}{X_4} - J_{11}\left[\frac{i(\Gamma_{23} - \Gamma_{24})}{X_4}C_2 - B_2\right]}{J_{21}J_{12} - J_{11}J_{22}},$$

$$a_{441}^{(2)} = \frac{-C_1 - X_1a_{111}^{(2)} - X_2a_{221}^{(2)}}{X_4},$$

$$a_{442}^{(2)} = \frac{-C_2 - X_1a_{112}^{(2)} - X_2a_{222}^{(2)}}{X_4},$$

$$a_{431}^{(2)} = \frac{1}{(\omega + d_{43})}\left[\Omega_c\left(a_{111}^{(2)} + a_{221}^{(2)} + 2a_{441}^{(2)}\right) + \frac{\Omega_c\left(\sigma_{11}^{(0)} - \sigma_{44}^{(0)}\right) + (\omega + d_{41}^*)\sigma_{43}^{(0)}}{D_1^*}\right],$$

$$a_{432}^{(2)} = \frac{1}{(\omega + d_{43})}\left[\Omega_c\left(a_{112}^{(2)} + a_{222}^{(2)} + 2a_{442}^{(2)}\right) + \frac{\Omega_c\left(\sigma_{22}^{(0)} - \sigma_{44}^{(0)}\right) + (\omega + d_{42}^*)\sigma_{43}^{(0)}}{D_2^*}\right],$$

where

$$A_1 = \frac{(\omega + d_{31})\left(\sigma_{11}^{(0)} - \sigma_{44}^{(0)}\right) + \Omega_c \sigma_{43}^{*(0)}}{D_1} - \frac{(\omega + d_{31}^*)\left(\sigma_{11}^{(0)} - \sigma_{44}^{(0)}\right) + \Omega_c^* \sigma_{43}^{(0)}}{D_1^*},$$

$$B_2 = \frac{(\omega + d_{32})\left(\sigma_{22}^{(0)} - \sigma_{44}^{(0)}\right) + \Omega_c \sigma_{43}^{*(0)}}{D_2} - \frac{(\omega + d_{32}^*)\left(\sigma_{22}^{(0)} - \sigma_{44}^{(0)}\right) + \Omega_c^* \sigma_{43}^{(0)}}{D_2^*},$$

$$C_1 = \frac{|\Omega_c|^2\left(\sigma_{11}^{(0)} - \sigma_{44}^{(0)}\right) + \Omega_c(\omega + d_{41})\sigma_{43}^{*(0)}}{D_1} - \frac{|\Omega_c|^2\left(\sigma_{11}^{(0)} - \sigma_{44}^{(0)}\right) + \Omega_c^*(\omega + d_{41}^*)\sigma_{43}^{(0)}}{D_1^*},$$

$$C_2 = \frac{|\Omega_c|^2\left(\sigma_{22}^{(0)} - \sigma_{44}^{(0)}\right) + \Omega_c(\omega + d_{42})\sigma_{43}^{*(0)}}{D_2} - \frac{|\Omega_c|^2\left(\sigma_{22}^{(0)} - \sigma_{44}^{(0)}\right) + \Omega_c^*(\omega + d_{42}^*)\sigma_{43}^{(0)}}{D_2^*}.$$

APPENDIX E: EXPLICT EXPRESSIONS OF W_{jl} IN EQ. (8)

$$W_{11} = -\kappa_{14}\frac{(\omega + d_{31})\left(a_{111}^{(2)} - a_{441}^{(2)}\right) + \Omega_c a_{431}^{*(2)}}{D_1}, \tag{E1a}$$

$$W_{12} = -\kappa_{14}\frac{(\omega + d_{31})\left(a_{112}^{(2)} - a_{442}^{(2)}\right) + \Omega_c a_{432}^{*(2)} + (\omega + d_{31})a_{21}^{(2)}}{D_1}, \tag{E1b}$$

$$W_{21} = -\kappa_{24}\frac{(\omega + d_{32})\left(a_{222}^{(2)} - a_{442}^{(2)}\right) + \Omega_c a_{432}^{*(2)} + (\omega + d_{32})a_{21}^{(2)}}{D_2}, \tag{E1c}$$

$$W_{22} = -\kappa_{24}\frac{(\omega + d_{32})\left(a_{221}^{(2)} - a_{441}^{(2)}\right) + \Omega_c a_{431}^{*(2)}}{D_2}, \tag{E1d}$$

where $a_{21}^{(2)} = ((\omega + d_{32}^*)\sigma_{22}^{(0)}/D_2^* - (\omega + d_{31}^*)\sigma_{11}^{(0)}/D_1^*)/(\omega + d_{21})$.

[1] M. Fleischhauer, A. Imamoglu, and J. P. Marangos, Rev. Mod. Phys. **77**, 633 (2005).
[2] S. E. Harris, Phys. Today **50**(7), 36 (1997).
[3] Z. Bai, C. Hang, and G. Huang, Chin. Opt. Lett. **11**, 012701 (2013).
[4] Y. Chen, Z. Bai, and G. Huang, Phys. Rev. A **89**, 023835 (2014).
[5] D. Petrosyan and Y. P. Malakyan, Phys. Rev. A **70**, 023822 (2004).
[6] S. Rebic, D. Vitali, C. Ottaviani, P. Tombesi, M. Artoni, F. Cataliotti, and R. Corbalan, Phys. Rev. A **70**, 032317 (2004).
[7] Z. B. Wang, K. P. Marzlin, and B. C. Sanders, Phys. Rev. Lett. **97**, 063901 (2006).
[8] S. Li, X. Yang, X. Cao, C. Zhang, C. Xie, and H. Wang, Phys. Rev. Lett. **101**, 073602 (2008).
[9] A. MacRae, G. Campbell, and A. I. Lvovsky, Opt. Lett. **33**, 2659 (2008).
[10] C. Hang and G. Huang, J. Opt. Soc. Am. B **26**, 413 (2009).
[11] L. Karpa, F. Vewinger, and M. Weitz, Phys. Rev. Lett. **101**, 170406 (2008).
[12] H.-H. Wang, Y.-F. Fan, R. Wang *et al.*, Opt. Lett. **34**, 2596 (2009).
[13] H. Wang, S. Li, Z. Xu, X. Zhao, L. Zhang, J. Li, Y. Wu, C. Xie, K. Peng, and M. Xiao, Phys. Rev. A **83**, 043815 (2011).
[14] S. Riedl, M. Lettner, C. Vo, S. Baur, G. Rempe, and S. Dürr, Phys. Rev. A **85**, 022318 (2012).
[15] J. Wu, Y. Liu, D.-S. Ding, Z.-Y. Zhou, B.-S. Shi, and G.-C. Guo, Phys. Rev. A **87**, 013845 (2013).
[16] R. W. Boyd, *Nonlinear Optics*, 3rd ed. (Academic Press, Elsevier, Waltham, 2008).
[17] G. Huang, L. Deng, and M. G. Payne, Phys. Rev. E **72**, 016617 (2005).
[18] The frequency and wave number of the probe field are given by $\omega_p + \omega$ and $k_p + K(\omega)$, respectively. Thus $\omega = 0$ corresponds to the center frequency of the probe field.
[19] M. Fleischhauer and M. D. Lukin, Phys. Rev. Lett. **84**, 5094 (2000).
[20] C. Liu, Z. Dutton, C. Behroozi, and L. Hau, Nature (London) **409**, 490 (2001).
[21] D. F. Phillips, A. Fleischhauer, A. Mair, R. L. Walsworth, and M. D. Lukin, Phys. Rev. Lett. **86**, 783 (2001).
[22] M. D. Eisaman, A. André, F. Massou, M. Fleischhauer, A. S. Zibrov, and M. D. Lukin, Nature (London) **438**, 837 (2005).
[23] J. J. Longdell, E. Fraval, M. J. Sellars, and N. B. Manson, Phys. Rev. Lett. **95**, 063601 (2005).
[24] U. Schnorrberger, J. D. Thompson, S. Trotzky, R. Pugatch, N. Davidson, S. Kuhr, and I. Bloch, Phys. Rev. Lett. **103**, 033003 (2009).
[25] R. Zhao, Y. O. Dudin, S. D. Jenkins, C. J. Campbel, D. N. Matsukevich, T. A. B. Kennedy, and A. Kuzmich, Nat. Phys. **5**, 95 (2009).

[26] R. Zhang, S. R. Garner, and L. V. Hau, Phys. Rev. Lett. **103**, 233602 (2009).
[27] A. G. Radnaev, Y. O. Dudin, R. Zhao, H. H. Jen, S. D. Jenkins, A. Kuzmich, and T. A. B. Kennedy, Nat. Phys. **6**, 894 (2010).
[28] Y. O. Dudin, R. Zhao, T. A. B. Kennedy, and A. Kuzmich, Phys. Rev. A **81**, 041805(R) (2010).
[29] F. Yang, T. Mandel, C. Lutz, Z.-S. Yuan, and J.-W. Pan, Phys. Rev. A **83**, 063420 (2011).
[30] I. Novikova, R. L. Walsworth, and Y. Xiao, Laser Photonics Rev. **6**, 333 (2012).
[31] H.-N. Dai, H. Zhang, S.-J. Yang, T.-M. Zhao, J. Rui, Y.-J. Deng, L. Li, N.-L. Liu, S. Chen, X.-H. Bao, X.-M. Jin, B. Zhao, and J.-W. Pan, Phys. Rev. Lett. **108**, 210501 (2012).
[32] Y. O. Dudin, L. Li, and A. Kuzmich, Phys. Rev. A **87**, 031801 (2013).
[33] G. Heinze, C. Hubrich, and T. Halfmann, Phys. Rev. Lett **111**, 033601 (2013).
[34] I. Novikova, N. B. Phillips, and A. V. Gorshkov, Phys. Rev. A **78**, 021802(R) (2008).
[35] R. Loudon, *The Quantum Theory of Light* (Oxford University Press, New York, 2000).
[36] L. G. Si, W. X. Yang, X. Y. Lu, X. Hao, and X. Yang, Phys. Rev. A **82**, 013836 (2010).
[37] D. A. Steck, http://steck.us/alkalidata/.
[38] G. Huang, C. Hang, and L. Deng, Eur. Phys. J. D **40**, 437 (2006).
[39] J. R. Morris and B. W. Shore, Phys. Rev. A **27**, 906 (1983).